Supplemental Experimental Procedures

Generation of bone marrow stromal cells. Bones from hips, tibia and femur were crushed with mortar and pestle into PBS with 2% FCS, filtered and plated in 75 cm^2 tissue culture flasks (BD Biosciences). Adherent cells were propagated for 10 days in α-MEM (Hyclone) with 20% FCS, then trypsinized, split and propagated for an additional 3 days. The cells were then trypsinzed and enriched for the mesenchymal stem cell marker CD105 (clone MJ7/18, Biolegend) using immunomagnetic positive selection (Life Technologies). The CD105-enriched fraction was then replated in flasks and used 3 - 7 days later for co-culture experiments.

Cell cycle and apoptosis analysis. For analysis of cell cycle, T-ALL cells were isolated ex vivo from the recipients that received a single i.p. injection of Bromodeoxyuridine (BrdU, Sigma-Aldrich) 45 minutes prior to sacrificing. MA9 AML cells growing in cytokine supplemented liquid culture were incubated with BrdU for 45 minutes. The cells were then fixed, permeabilized and stained with APC-conjugated anti-BrdU antibody (clone PRB-1) and DAPI. For quantification of apoptosis, cells were stained with APC-conjugated Annexin V (BD Pharmingen) and either DAPI or propidium iodide.

Production of retroviral and lentiviral supernatant. The MSCV-based retroviral constructs included the human MLL-AF9 fusion oncogene and neomycin resistance gene (Somervaille and Cleary, 2006); bicistronic Hoxa9-IRES-Meis1 (Lessard and Sauvageau, 2003), NotchIC-IRES-GFP (Pui et al., 1999) and Myc-IRES-GFP (Hemann et al., 2005). HEK-293T cells for retroviral and lentiviral production were maintained in DMEM with 10% FCS. Ecotropic retroviral supernatant was generated by co-transfection of 293T cells using the lipid-based transfection reagent TransIT 293 (Mirus Bio LLC, Madison, WI) with three plasmids containing the MSCV retroviral expression constructs, the ecotropic envelope and packaging components.

TRC shRNA lentiviral constructs in the pLKO.1 backbone were purchased from Open-Biosystems and Sigma-Aldrich. A pLKO.1 'scramble' shRNA for use as a hairpin control was obtained from Addgene (Sarbassov et al., 2005). An additional lentiviral shRNA (Sh3) was used to knockdown ZFX in human cells, and this construct expressed GFP as a selectable marker. This third-generation lentiviral vector was modified to express shRNAs from the H1 promoter as previously described (Fasano et al., 2007). For experiments using Sh3, transduced NOMO-1 cells were sorted to select for GFP^+ shRNA-expressing cells.

Retroviral transduction of hematopoietic progenitors. Hematopoietic progenitors were isolated by flushing the bone marrow from the long bones, followed by red blood cell lysis and immunomagnetic positive selection (Miltenyi Biotec, Auburn, CA) using c-Kit antibody (clone 2B8, eBioscience, San Diego, CA). These progenitors were then spin infected in 7-8 separate wells of 6-well plates (1300g X 90 minutes) with 7 µg/ml Polybrene (Sigma-Aldrich, St. Louis, MO) in 1 part retroviral supernatant and 3 parts R20 AML media. Following repeat spin infections at 24 hours and 48 hours post isolation, the cells from each well were washed in PBS and injected i.v. into sublethally irradiated recipient mice.

Microarray analysis. Lists of Zfx-dependent genes were generated using the web-based NIA Array analysis software running ANOVA (Sharov et al., 2005). Gene Set Enrichment Analysis was performed using GSEA v2.07 software according to the developers' recommendations (Subramanian et al., 2005). Public microarray data for GSEA included the Immgen dataset of murine hematopoietic cell subsets (Heng and Painter, 2008) (GSE15907) and the analysis of Myc inhibition in murine AML cells (Zuber et al., 2011) (GSE29799). Proliferation signature gene sets were derived by querying the Immgen (Heng and Painter, 2008) and BioGPS (Wu et al., 2009) expression databases for the probes that correlate with the proliferation marker Mki67.

For the analysis of Myc overexpression, expression data were obtained for three biological replicas of four progenitor cell samples: wild-type overexpressing GFP (WT), Zfx knockout overexpressing GFP (ΔZfx), wild-type overexpressing Myc (Myc) and Zfx knockout overexpressing Myc (ΔZfxMyc). Expression values for each probe were $\log_2$-transformed and then averaged over replicas. To find differentially expressed probes, we considered Myc vs WT and ΔZfx vs WT test-control pairs and used method from (Galan-Caridad et al., 2007) to compute P-values and E-values (the expected number of false positives); and identified differentially expressed probes as E<0.5 (E<5 for Myc response). We further selected probes that show at least 1.5-fold difference in expression. Next, we indentified probes that respond to Myc differently in WT and in ΔZfx. First, we computed expected response to both ΔZfx and Myc assuming their independent effects as Expected=ΔZfx+Myc-WT. Second, we compacted Expected to Observed=ΔZfxMyc expression and found that most of the gene respond independently (correlation(Expected,Observed)=0.998 with the regression slope beta=1±0.0002), allowing to use residuals in this regression to identify non-independent response to Myc and ΔZfx. We further verified that these residuals (i.e. Expected-Observed values) do not depend on expression values in individual experiments (Myc, WT, ΔZfx, correlation<0.1). We next found probes that responded non-independently to Myc and ΔZfx by applying our procedure for finding differentially expressed probes (Galan-Caridad et al., 2007) to Observed vs Expected values.

ChIP-Seq analysis. Sequencing reads were aligned to the human genome (UCSC hg19) and the mouse genome (UCSC mm10) using the short read aligner Bowtie version 2.0 (Langmead et al., 2009). Significantly enriched ChIP regions were identified using the Model-based analysis of ChIP-Seq (MACS) version 1.4 (Zhang et al., 2008). The absolute distances between significant peaks and their nearest TSS was calculated using PeakAnnotator 1.4 (Salmon-Divon et al., 2010). These regions of enrichment were visualized using DNAnexus (Mt. View, CA). Overlap between gene lists was assessed and graphically depicted using BioVenn (Hulsen et al., 2008). The analysis of genome features within ZFX binding sites was done using the Cis-regulatory Element Annotation System (CEAS) (Shin et al., 2009). Gene Ontology analysis was performed using DAVID Bioinformatics Resources version 6.7 (Huang da et al., 2009).

Previously reported Zfx ChIP-seq data from murine ESCs were downloaded from the NCBI Sequence Read Archive (SRX000552) (Chen et al., 2008). The binding data for Myc in K562 cells were from the ENCODE consortium (GEO accession number GSE31477).

Supplemental References

Chen, X., Xu, H., Yuan, P., Fang, F., Huss, M., Vega, V.B., Wong, E., Orlov, Y.L., Zhang, W., Jiang, J.*, et al.* (2008). Integration of external signaling pathways with the core transcriptional network in embryonic stem cells. Cell *133*, 1106-1117.

Fasano, C.A., Dimos, J.T., Ivanova, N.B., Lowry, N., Lemischka, I.R., and Temple, S. (2007). shRNA knockdown of Bmi-1 reveals a critical role for p21-Rb pathway in NSC self-renewal during development. Cell Stem Cell *1*, 87-99.

Galan-Caridad, J.M., Harel, S., Arenzana, T.L., Hou, Z.E., Doetsch, F.K., Mirny, L.A., and Reizis, B. (2007). Zfx controls the self-renewal of embryonic and hematopoietic stem cells. Cell *129*, 345-357.

Hemann, M.T., Bric, A., Teruya-Feldstein, J., Herbst, A., Nilsson, J.A., Cordon-Cardo, C., Cleveland, J.L., Tansey, W.P., and Lowe, S.W. (2005). Evasion of the p53 tumour surveillance network by tumour-derived MYC mutants. Nature *436*, 807-811.

Heng, T.S., and Painter, M.W. (2008). The Immunological Genome Project: networks of gene expression in immune cells. Nat Immunol *9*, 1091-1094.

Huang da, W., Sherman, B.T., and Lempicki, R.A. (2009). Systematic and integrative analysis of large gene lists using DAVID bioinformatics resources. Nat Protoc *4*, 44-57.

Hulsen, T., de Vlieg, J., and Alkema, W. (2008). BioVenn - a web application for the comparison and visualization of biological lists using area-proportional Venn diagrams. BMC Genomics *9*, 488.

Langmead, B., Trapnell, C., Pop, M., and Salzberg, S.L. (2009). Ultrafast and memory-efficient alignment of short DNA sequences to the human genome. Genome Biol *10*, R25.

Lessard, J., and Sauvageau, G. (2003). Bmi-1 determines the proliferative capacity of normal and leukaemic stem cells. Nature *423*, 255-260.

Lukk, M., Kapushesky, M., Nikkila, J., Parkinson, H., Goncalves, A., Huber, W., Ukkonen, E., and Brazma, A. (2010). A global map of human gene expression. Nat Biotechnol *28*, 322-324.

Pui, J.C., Allman, D., Xu, L., DeRocco, S., Karnell, F.G., Bakkour, S., Lee, J.Y., Kadesch, T., Hardy, R.R., Aster, J.C.*, et al.* (1999). Notch1 expression in early lymphopoiesis influences B versus T lineage determination. Immunity *11*, 299-308.

Salmon-Divon, M., Dvinge, H., Tammoja, K., and Bertone, P. (2010). PeakAnalyzer: genome-wide annotation of chromatin binding and modification loci. BMC Bioinformatics *11*, 415.

Sarbassov, D.D., Guertin, D.A., Ali, S.M., and Sabatini, D.M. (2005). Phosphorylation and regulation of Akt/PKB by the rictor-mTOR complex. Science *307*, 1098-1101.

Sharov, A.A., Dudekula, D.B., and Ko, M.S. (2005). A web-based tool for principal component and significance analysis of microarray data. Bioinformatics *21*, 2548-2549.

Shin, H., Liu, T., Manrai, A.K., and Liu, X.S. (2009). CEAS: cis-regulatory element annotation system. Bioinformatics *25*, 2605-2606.

Somervaille, T.C., and Cleary, M.L. (2006). Identification and characterization of leukemia stem cells in murine MLL-AF9 acute myeloid leukemia. Cancer Cell *10*, 257-268.

Subramanian, A., Tamayo, P., Mootha, V.K., Mukherjee, S., Ebert, B.L., Gillette, M.A., Paulovich, A., Pomeroy, S.L., Golub, T.R., Lander, E.S.*, et al.* (2005). Gene set enrichment analysis: a knowledge-based approach for interpreting genome-wide expression profiles. Proc Natl Acad Sci U S A *102*, 15545-15550.

Wu, C., Orozco, C., Boyer, J., Leglise, M., Goodale, J., Batalov, S., Hodge, C.L., Haase, J., Janes, J., Huss, J.W., 3rd*, et al.* (2009). BioGPS: an extensible and customizable portal for querying and organizing gene annotation resources. Genome Biol *10*, R130.

Zhang, Y., Liu, T., Meyer, C.A., Eeckhoute, J., Johnson, D.S., Bernstein, B.E., Nusbaum, C., Myers, R.M., Brown, M., Li, W.*, et al.* (2008). Model-based analysis of ChIP-Seq (MACS). Genome Biol *9*, R137.

Zuber, J., Shi, J., Wang, E., Rappaport, A.R., Herrmann, H., Sison, E.A., Magoon, D., Qi, J., Blatt, K., Wunderlich, M.*, et al.* (2011). RNAi screen identifies Brd4 as a therapeutic target in acute myeloid leukaemia. Nature *478*, 524-528.

Supplemental Figures

Figure S1. Zfx facilitates proliferation of immature thymocytes but is dispensable for normal T cell development (Related to Fig. 1).
(A) Zfx deletion during embryonic and postnatal thymopoiesis in the *Tie2*-Cre$^+$ *Zfx*^{fl}/y pan-hematopoietic conditional knockout (CKO) mice. Zfx deletion was analyzed by genomic PCR in 16.5 d.p.c. fetal livers or in spleens (S), thymi (T) and bone marrow (B) of postnatal CKO mice or Cre-negative littermate controls (Ctrl). Bands corresponding to wild-type (wt), unrecombined (flox) and recombined (null) alleles of Zfx are indicated.
(B) Thymocyte development in *Tie2*-Cre CKO mice with pan-hematopoietic Zfx deletion. Shown are staining profiles of fetal (15.5-18.5 d.p.c.) or newborn (day 2) thymocytes from CKO or littermate control (Ctrl) mice.
(C) Thymocyte proliferation at the DN to DP transition in *Tie2*-Cre CKO mice. Young (3-wk old) CKO or littermate control (Ctrl) mice were injected with BrdU and analyzed 1 hr later. Shown are BrdU and DNA content (7-AAD) staining profiles of DN4 and ISP thymocytes, as well as Lin$^-$ Sca-1$^-$ c-Kit$^+$ erythromyeloid progenitors (EMP) from the BM. Similar results were obtained in adult *R26*-CreER$^+$ *Zfx*^{fl}/y mice after tamoxifen-induced Zfx deletion in vivo (not shown).
(D-E) Thymocyte development after Zfx deletion at the DN-to-DP transition. Shown are staining profiles of thymocytes from adult *CD4*-Cre$^+$ *Zfx*^{fl}/y (CKO) or littermate control (Ctrl) mice (D), and cell numbers of different thymocyte subsets including DN, DP and SP CD4$^+$ and CD8$^+$ thymocytes (E, mean ± SEM of 5-6 animals).

Figure S2. Inducible deletion of Zfx in NotchIC-driven T-ALL (related to Figure 2).
(A) Characterization of pre-established T-ALL in secondary recipient mice. Shown is representative CD4/CD8 staining of the total BM from a healthy control and a moribund recipient of *Zfx*^{fl}*/y* T-ALL cells.
(B) Genomic PCR for Cre-mediated recombination at the floxed *Zfx* locus. Shown are representative PCR products from *Zfx*^{fl}*/y* T-ALL cells that were sorted from recipients that were untreated or treated with Tmx 5 days before.
(C) The effect of *Zfx* deletion on the expression of Notch target genes in NotchIC-induced T-ALL. *R26*-CreER$^+$ *Zfx*^{wt}/y or *Zfx*^{fl}/y T-ALL cells were sorted from secondary recipients 5 days after the treatment with Tmx or vehicle. Shown are relative expression levels in arbitrary units as determined by qRT-PCR (mean ± SEM of 5 independent lines).
(D) The cell cycle status of T-ALL cells after Zfx deletion. Recipients of *R26*-CreER$^+$ *Zfx*^{fl}/y T-ALL cells were treated with Tmx or vehicle, and 5 days later they were injected with BrdU and sacrificed 1 hour later. Shown are staining profiles for DNA content (DAPI) and DNA synthesis (BrdU) of gated GFP+ T-ALL cells, with the G0/G1, S and G2/M cell cycle phases highlighted. Representative of 3 independent experiments.
(E) The survival of T-ALL cells after Zfx deletion. Cells isolated as in panel D were stained for permeability (Propidium iodide) and surface phosphatidylserine (Annexin V). Shown are staining profiles of gated GFP+ T-ALL cells, with the late apoptotic cells highlighted.

Figure S3. Inducible deletion of Zfx in murine MA9-induced AML (related to Figure 3).

(A) The effect of *Zfx* deletion on the cell cycle status of MA9 AML cells. *R26*-CreER^{+} *Zfx*^{wt}/y or *Zfx*^{fl}/y MA9 AML cells were grown in cytokine-supplemented liquid media with 4-OHT or vehicle for 3 days, and their cell cycle status was analyzed by BrdU incorporation as in Fig. S2D. Shown is the fraction of cells in the indicated phases of cell cycle (mean ± S.E.M. of 3-5 independent lines)

(B) The effect of Zfx deletion on the surface phenotype of MA9 AML cells. *R26*-CreER^{+} *Zfx*^{wt}/y or *Zfx*^{fl}/y MA9 AML cells were grown in cytokine-supplemented liquid media with 4-OHT for 72 hours, and analyzed after additional 4 days of culture. The fraction of immature c-Kit^{+} CD14^{-} AML cells is indicated (mean ± S.E.M. of 5-6 independent lines).

(C) The effect of *Zfx* deletion on the expression of functional transcription factors in AML. Shown are relative expression levels in arbitrary units as determined by qRT-PCR in AML cells described in panel A (mean ± SEM of 7 independent lines).

(D) Overexpression of *Six1* and *Frzb* in an AML cell line that displays partial dependence on Zfx. Shown are relative expression levels in arbitrary units as determined by qRT-PCR in five independent MLL-AF9 AML cell lines (mean ± SEM of triplicate PCR reactions).

Figure S4. Zfx is enriched in human leukemias and facilitates the growth of human leukemia cell lines (related to Figure 4).

(A) The expression of human ZFX and its gametolog ZFY in normal human and malignant tissue samples. Expression levels of three Affymetrix microarray probes for ZFX and one for ZFY are based on (Lukk et al., 2010) and presented as an output from the associated web interface (http://www.ebi.ac.uk/gxa/array/U133A). The "leukemia" metagroup is indicated among 15 metagroups of normal and neoplastic tissues samples, and the significance of enrichment in this metagroup is indicated.

(B-C) The effect of ZFX knockdown on the growth of human T-ALL line RPMI-8402 (panel B) and AML line NOMO-1 (panel B). Cells were transduced with lentiviral constructs encoding control scrambled shRNA (Scr) or two shRNAs to ZFX (sh1-2) and selected. Shown are Western blots of ZFX protein level and a loading control (tubulin, TUB) after selection, and the cumulative cell numbers after growth for 2-3 passages. ** P<0.01 compared to scrambled shRNA.

(D) The knockdown of Zfx using an additional shRNA (Sh3) in a lentiviral vector with GFP expression. NOMO-1 cells were transduced with empty vector expressing either GFP only (GFP), control non-targeting shRNA (Ctrl) or shRNA against ZFX (sh3), and sorted for GFP expression. Shown are the Western blots of ZFX protein level and a loading control (tubulin, TUB), and the cumulative cell numbers after growth for 3 passages. ** P< 0.01 compared to control shRNA.

(E) The effect of ZFX knockdown on the growth of human AML line THP-1 and T-ALL lines CCRF-CEM and Jurkat. Cells were transduced and selected as in panels B-C. Shown are the cumulative cell numbers after growth for 2 passages.

(F) The effect of ZFX knockdown on the phenotype of NOMO-1 cells. Shown are representative staining profiles of c-Kit versus CD14 expression and the fraction of c-Kit^{+} CD14^{-} population in NOMO-1 cells 5 days after selection (mean ± SEM of 3 experiments); ** P< 0.01.

Figure S5. Characterization of Zfx target genes in T-ALL and AML (related to Figure 5).
(A) The distance of ZFX binding regions from the TSS of the corresponding target genes. The histogram depicts the distribution of distances between ZFX binding peaks determined by ChIP-Seq and the nearest TSS in human T-ALL line RPMI-8402 and AML line NOMO-1.
(B) The comparison of Zfx-controlled target genes with proliferation-associated genes. Gene sets directly activated by Zfx in T-ALL and AML (Fig. 6) were compared with "proliferation signature" gene sets derived from the Immgen and BioGPS expression databases. Shown are non-proportional Venn diagrams of the overlap between the datasets.
(C) The enrichment of Zfx target genes in T-ALL in normal immature thymocytes. GSEA for direct Zfx-activated target gene set defined in T-ALL was performed on normal thymocyte DN3a (quiescent) and DN3b/DN4 (proliferating) DN subsets compared to the more differentiated DP subset. Similar analysis for the "proliferation signature" genes is shown for comparison. Normal gene expression profiles were taken from the Immgen database.

Figure S6. Microarray analysis of gene expression in Myc-overexpressing progenitors (related to Figure 6).
Wild-type or Zfx-deficient myeloid progenitors transduced with Myc/GFP or GFP only were cultured for 4 days and analyzed by microarray (3 independent cultures for each sample). Average differential expression in Myc-expressing versus GFP-expressing cells of each Zfx genotype (Myc response) was calculated for each probe.
(A) Response to Myc overexpression in Zfx-deficient progenitors. Shown is the pairwise comparison of Myc responses in wild-type versus Zfx-deficient cells, with the probes showing differential responses in blue. The probes whose levels were decreased by Myc in wild-type cells are circled in purple.
(B) Response to Zfx deletion in Myc-overexpressing progenitors. Shown is the pairwise comparison of the effect of Zfx loss in Myc-expressing versus GFP-expressing progenitors, with the probes showing differential responses in blue. The probes whose levels were decreased in Zfx-deficient progenitors expressing GFP are circled in green.

Figure S7. The role of Zfx targets Idh2 and Ptpmt1 in murine AML (related to Figure 7).
(A) The binding of Zfx and Myc to the promoters of *Idh2* and *Ptpmt1* in murine ESCs. Shown are enrichment peaks for Zfx and Myc from the parallel ChIP-Seq analysis (Chen et al., 2008) for *Ptpmt1*, *Idh2*, *Eif4e2* (a prototype common target of Zfx and Myc) and *Dis3l* (a prototype target of Zfx but not Myc). The factor-gene interaction scores assigned in the study are shown. CpG islands are indicated in orange.
(B) The binding of ZFX and MYC to the promoters of *IDH2* and *PTPMT1* in human leukemia cells. Shown are ChIP enrichment peaks for ZFX in NOMO-1 AML line and RPMI-8402 T-ALL line (this study) and for MYC in K562 CML cell line (the ENCODE project).
(C) The effect of Idh2 knockdown on the growth of murine MA9-induced AML. AML cells expressing red fluorescent protein (dsRed) were transduced with lentiviral constructs encoding a control shRNA against GFP or three shRNA (sh1-3) against *Idh2*, and

selected with puromycin. Cells were grown on BM stromal cells for 4 days and counted; data represent mean SEM of triplicate cultures. * P< 0.05, ** P<0.01.
(D) The deletion of Zfx in *R26*-CreER^{+} *Zfx^{fl}/y* AML cells overexpressing Idh2 and Ptpmt1. Shown is genomic PCR for unrecombined (flox) and recombined (null) Zfx alleles in the BM of two moribund mice that have received AML cells shown in Fig. 8G.

Supplemental Tables

All tables are combined in a single Excel file

Table S1. Differentially expressed genes after Zfx deletion in murine T-ALL or AML cells (related to Figure 5).

Table S2. The distribution of ZFX binding peaks in the genome (related to Figure 5).

Table S3. ZFX ChIP-seq peaks within 1 Kb of annotated genes in RPMI-8402 or NOMO-1 human leukemia cells or in murine ESCs (related to Figure 5).

Table S4. Direct target genes of Zfx in leukemia (related to Figure 5).
Genes that are positively regulated by Zfx in murine T-ALL or AML cells and have Zfx ChIP-seq peaks within 1 Kb of the TSS in the corresponding human leukemia cells (RPMI-8402 or NOMO-1, respectively) are listed. The target genes in AML that overlap with those in T-ALL are indicated with the asterisk.

Table S5. Proliferation signature gene sets derived from the Immgen and BioGPS databases (related to Figure S5).

Table S6. The response to Myc in Zfx-deficient myeloid progenitors (related to Figure 6).
Shown are results of microarray analysis of wild-type (WT) or Zfx-deficient (KO) myeloid progenitors overexpressing Myc or GFP, including all probes that were significantly affected by Myc overexpression in WT cells, and those whose response to Myc was different in KO cells. Average Log_2 signals, P- and E-values of response to Myc and P- and E-values of differential response to Myc in KO cells are indicated for each probe.

Table S7. The effect of Zfx deficiency in Myc-overexpressing myeloid progenitors (related to Figure 6).
Shown are results of microarray analysis of wild-type (WT) or Zfx-deficient (KO) myeloid progenitors overexpressing Myc or GFP, including all probes that were significantly affected by Zfx deficiency in GFP-overexpressing cells, and those whose response to Zfx loss was different in Myc-overexpressing cells. Average Log_2 signals, P- and E-values of response to Zfx loss and P- and E-values of differential response to Zfx loss in Myc-overexpressing are indicated for each probe.

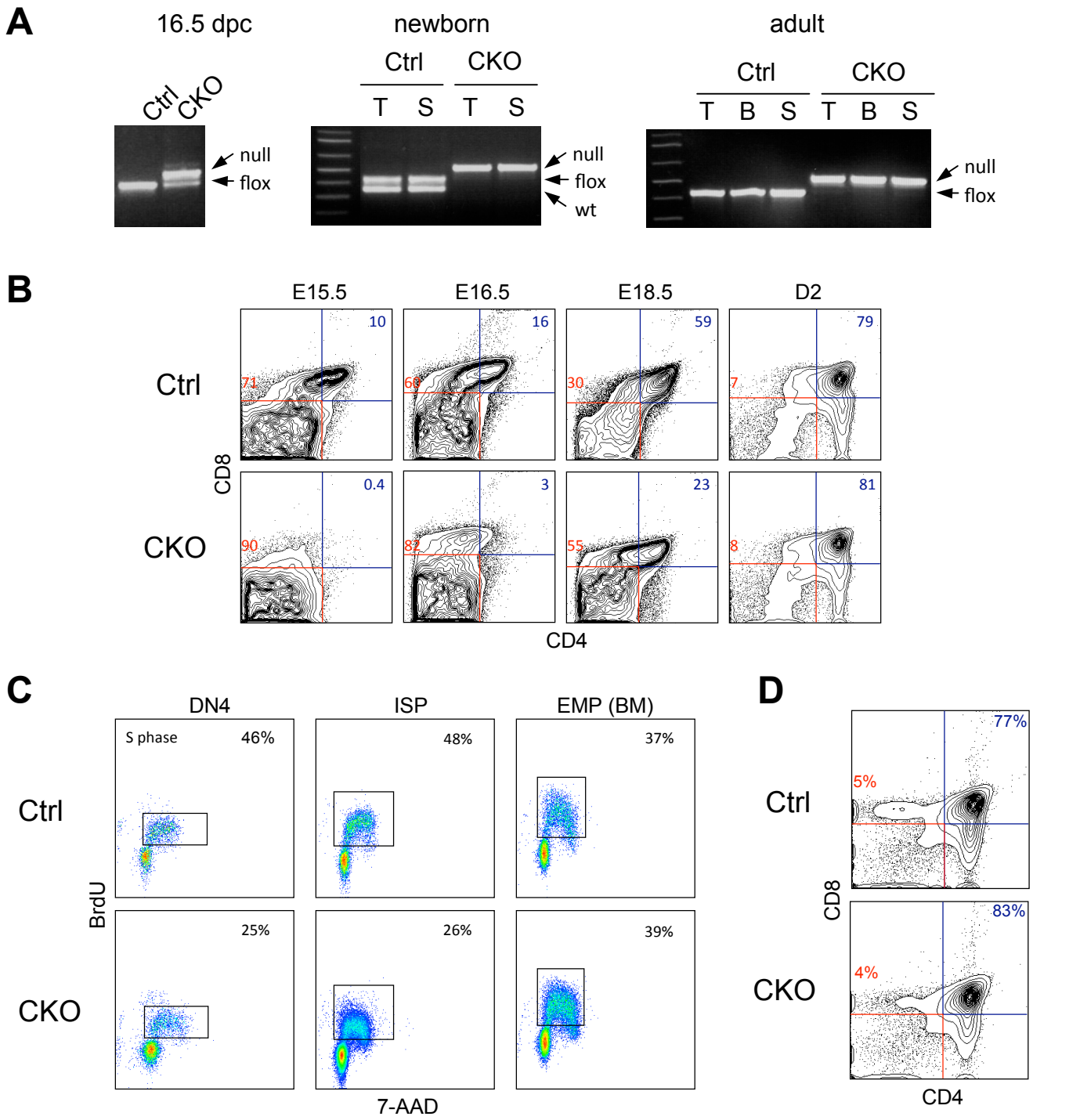
A
16.5 dpc
Ctrl
CKO
null
flox
newborn
Ctrl
CKO
T S T S
null
flox
wt
adult
Ctrl
CKO
T B S T B S
null
flox
B
E15.5
E16.5
E18.5
D2
Ctrl
CKO
CD8
10
71
16
68
59
30
79
7
0.4
90
3
82
23
55
81
8
CD4
C
DN4
ISP
EMP (BM)
Ctrl
CKO
S phase
46%
48%
37%
25%
26%
39%
BrdU
7-AAD
D
Ctrl
CKO
77%
5%
83%
4%
CD8
CD4
E
Cells, 10^6
200
150
100
50
0
Total
DP
Cells, 10^5
140
120
100
80
60
40
20
0
DN
CD4
CD8
Ctrl
CKO

Fig. S1

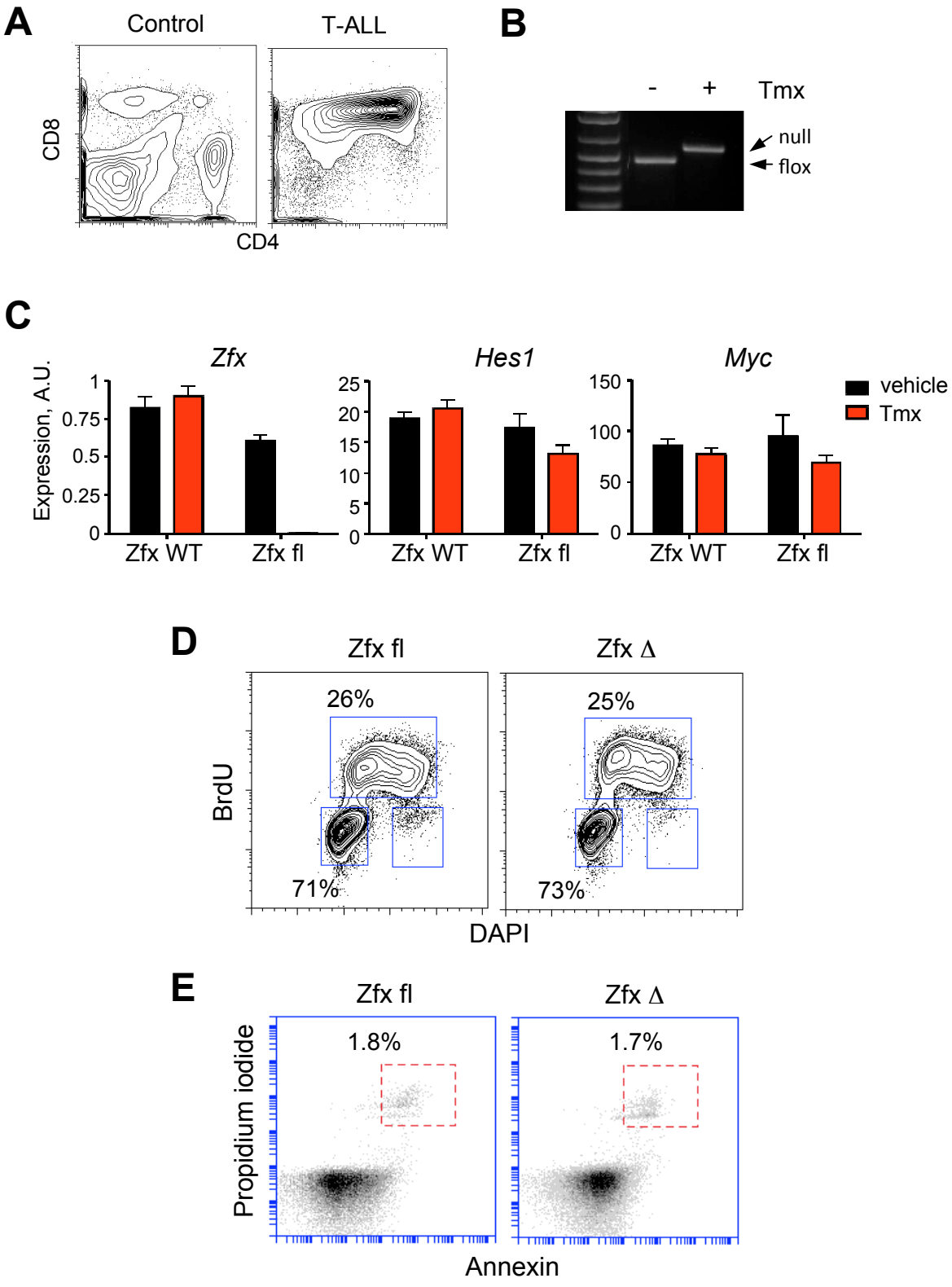
A
Control
T-ALL
CD8
CD4
B
-
+
Tmx
null
flox
C
Zfx
Hes1
Myc
Expression, A.U.
vehicle
Tmx
Zfx WT
Zfx fl
D
Zfx fl
Zfx Δ
26%
25%
71%
73%
BrdU
DAPI
E
Zfx fl
Zfx Δ
1.8%
1.7%
Propidium iodide
Annexin

Fig. S2

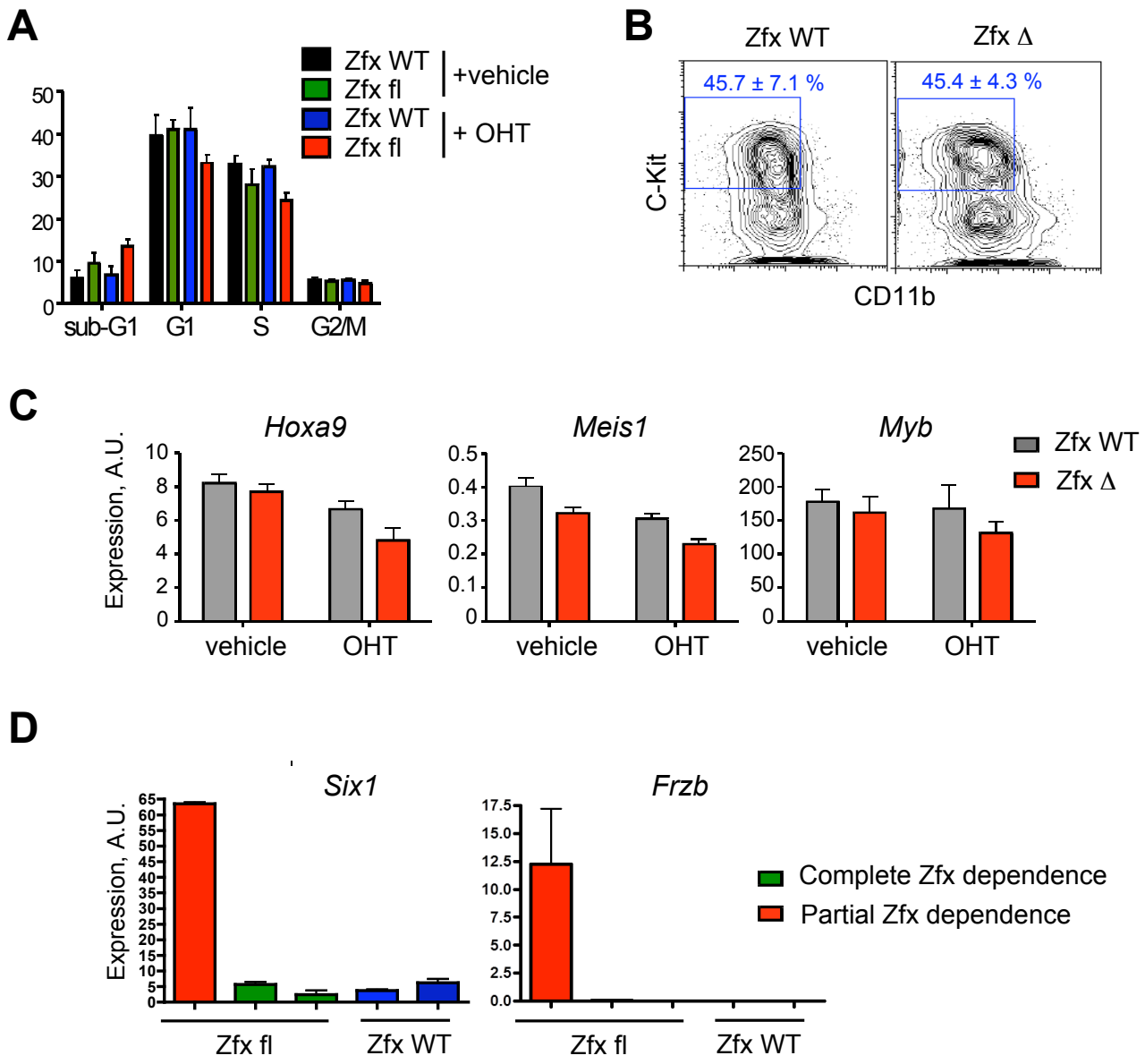
A
Zfx WT
Zfx fl
Zfx WT
Zfx fl
+vehicle
+ OHT
50
40
30
20
10
0
sub-G1
G1
S
G2/M
B
Zfx WT
Zfx Δ
45.7 ± 7.1 %
45.4 ± 4.3 %
C-Kit
CD11b
C
Hoxa9
Meis1
Myb
Expression, A.U.
vehicle
OHT
Zfx WT
Zfx Δ
D
Six1
Frzb
Expression, A.U.
Zfx fl
Zfx WT
Complete Zfx dependence
Partial Zfx dependence

Fig. S3

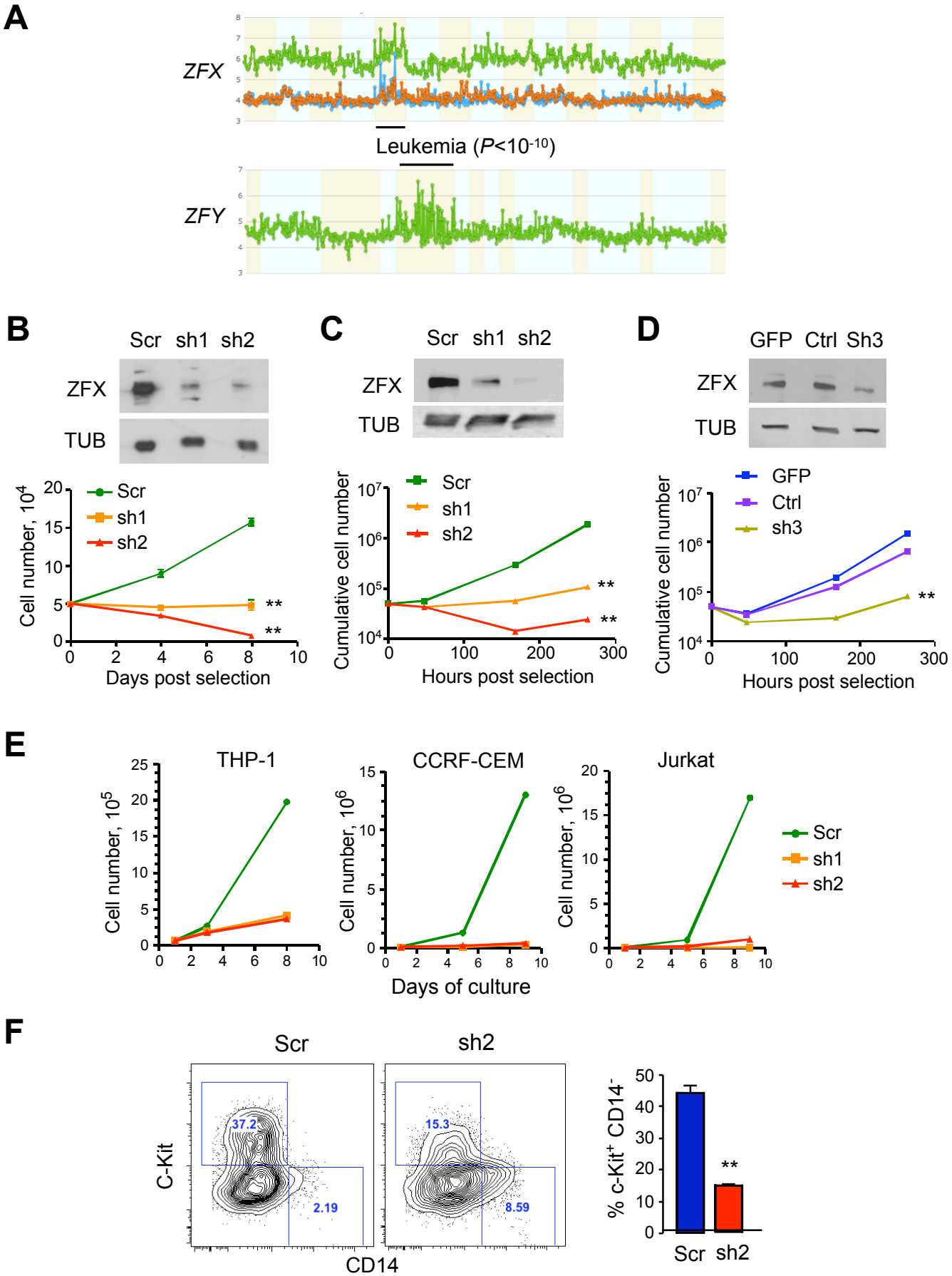
A
ZFX
Leukemia ($P<10^{-10}$)
ZFY
B
Scr sh1 sh2
ZFX
TUB
Cell number, 10^4
Scr
sh1
sh2
**
**
Days post selection
C
Scr sh1 sh2
ZFX
TUB
Cumulative cell number
Scr
sh1
sh2
**
**
Hours post selection
D
GFP Ctrl Sh3
ZFX
TUB
Cumulative cell number
GFP
Ctrl
sh3
**
Hours post selection
E
THP-1
CCRF-CEM
Jurkat
Cell number, 10^5
Cell number, 10^6
Cell number, 10^6
Scr
sh1
sh2
Days of culture
F
Scr
sh2
C-Kit
CD14
37.2
2.19
15.3
8.59
% c-Kit+ CD14-
**
Scr sh2

Fig. S4

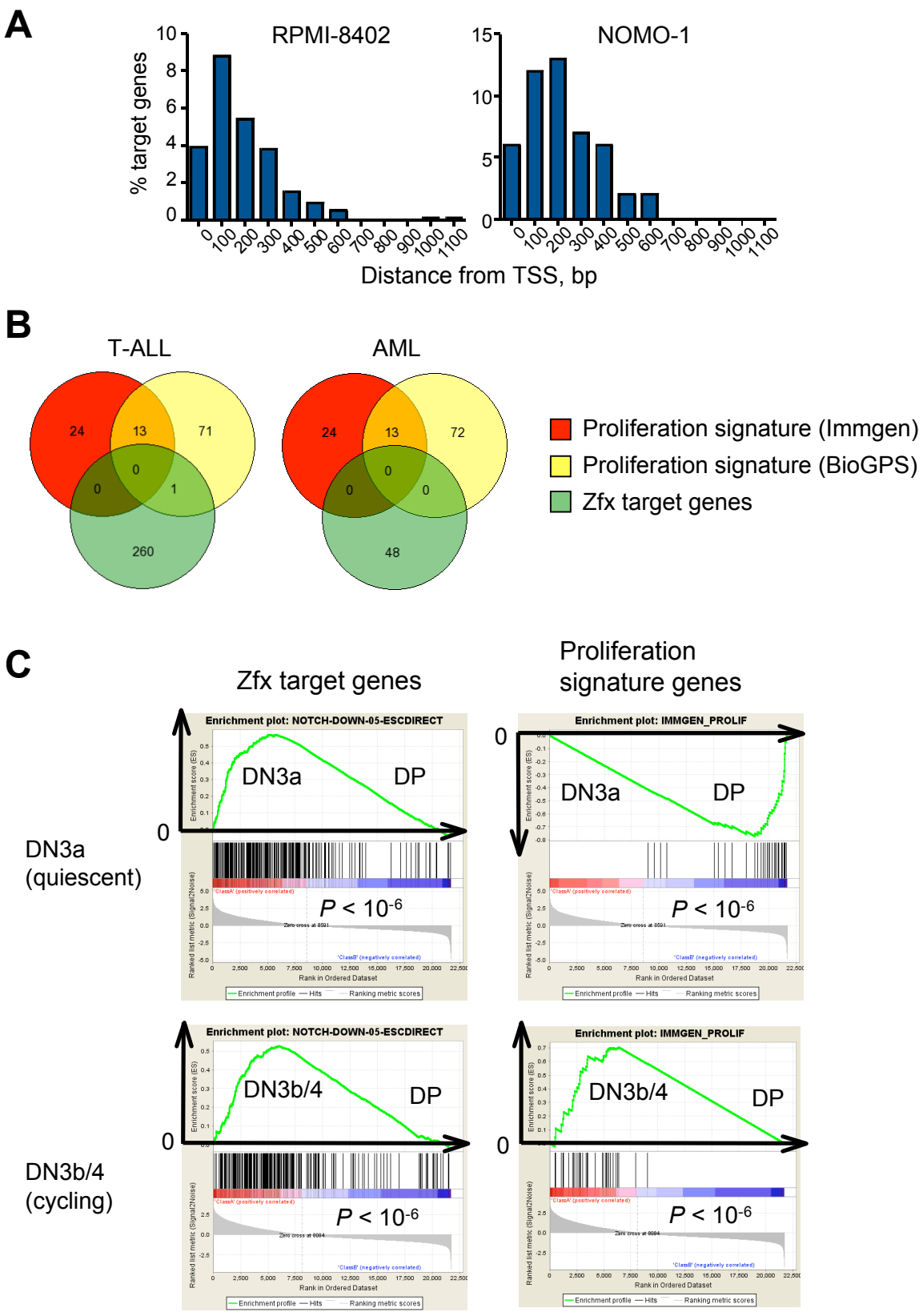
A
RPMI-8402
NOMO-1
% target genes
Distance from TSS, bp
B
T-ALL
AML
24
13
71
0
0
1
260
24
13
72
0
0
0
48
Proliferation signature (Immgen)
Proliferation signature (BioGPS)
Zfx target genes
C
Zfx target genes
Proliferation signature genes
DN3a (quiescent)
DN3b/4 (cycling)
Enrichment plot: NOTCH-DOWN-05-ESCDIRECT
Enrichment plot: IMMGEN_PROLIF
DN3a
DP
DN3b/4
DP
P < 10-6
Rank in Ordered Dataset
Enrichment profile
Hits
Ranking metric scores

Fig. S5

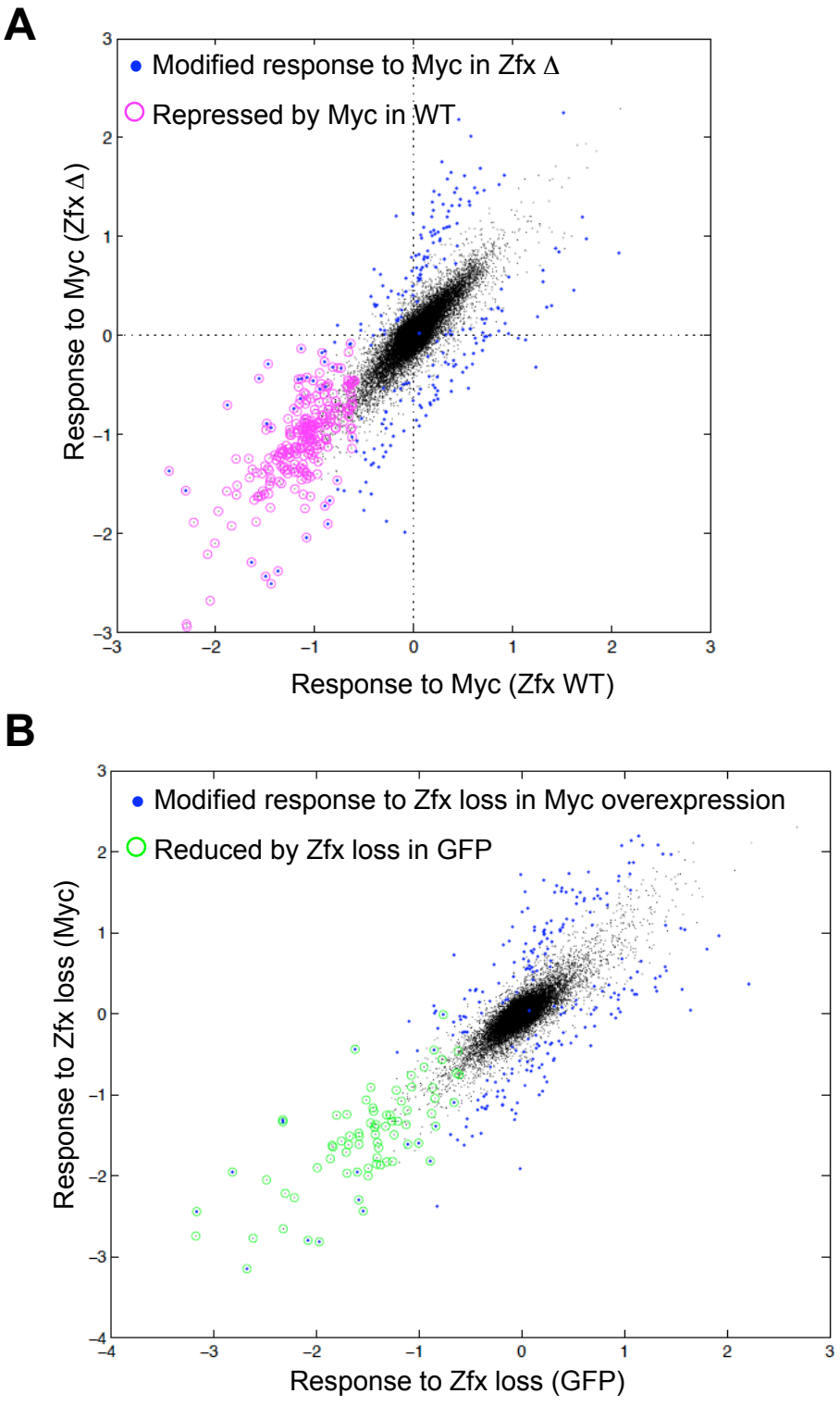
A
Modified response to Myc in Zfx Δ
Repressed by Myc in WT
Response to Myc (Zfx Δ)
Response to Myc (Zfx WT)
B
Modified response to Zfx loss in Myc overexpression
Reduced by Zfx loss in GFP
Response to Zfx loss (Myc)
Response to Zfx loss (GFP)

Fig. S6

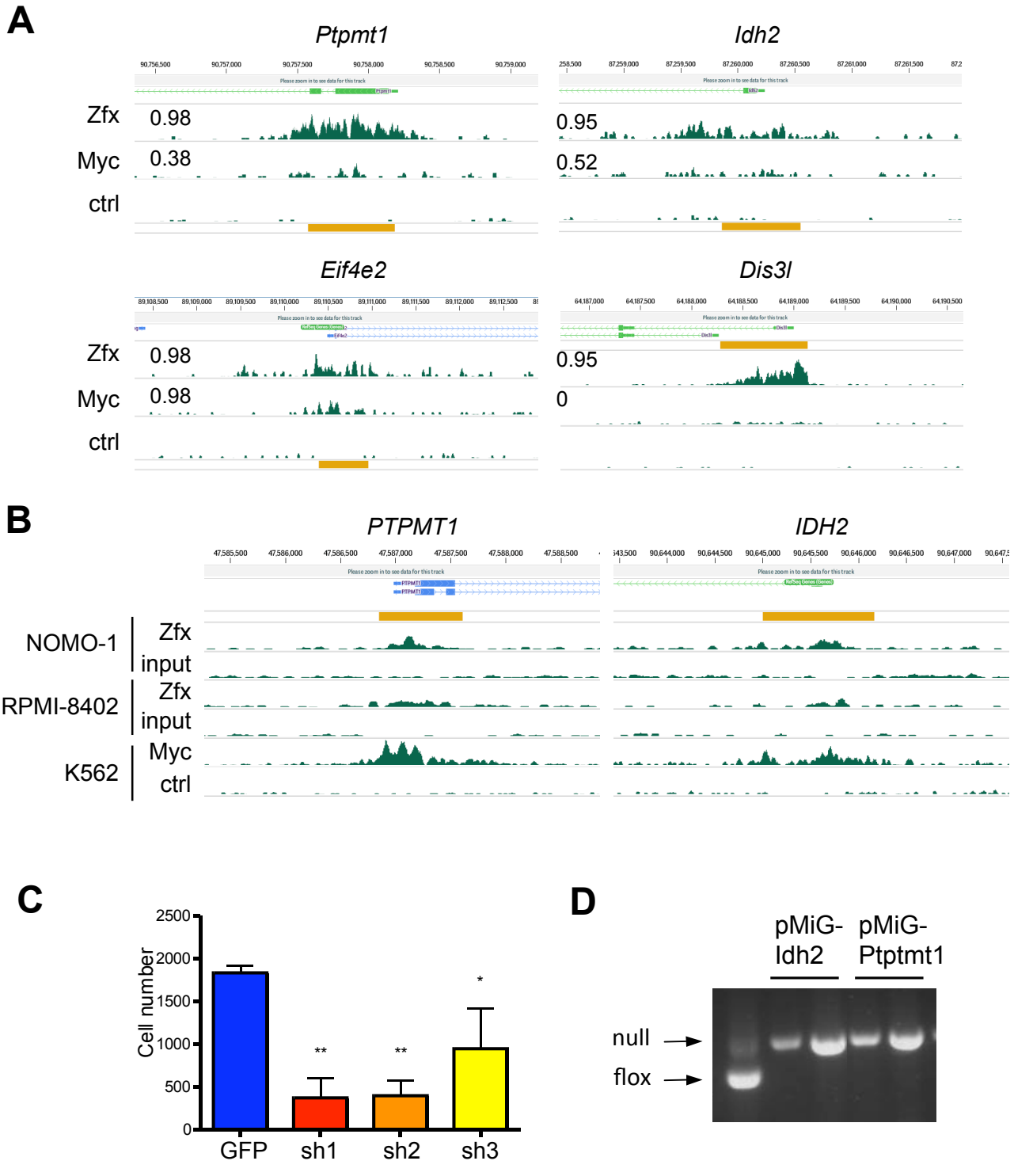
A
Ptpmt1
Idh2
Zfx
Myc
ctrl
0.98
0.38
0.95
0.52
Eif4e2
Dis3l
0.98
0.98
0.95
0
B
PTPMT1
IDH2
NOMO-1
RPMI-8402
K562
Zfx
input
Myc
ctrl
C
Cell number
2500
2000
1500
1000
500
0
GFP
sh1
sh2
sh3
**
**
*
D
pMiG-Idh2
pMiG-Ptptmt1
null
flox

Fig. S7